AGU PUBLICATIONS

Geophysical Research Letters

RESEARCH LETTER
10.1002/2013GL058777

Key Points:
- Seasonal sea level changes in the Gulf of Mexico are investigated
- A significant increase in the annual amplitude is found for the recent past
- Seasonal changes have exacerbated the flood risk in the eastern Gulf

Supporting Information:
- Readme
- Figure S1
- Figure S2
- Figure S3

Correspondence to:
T. Wahl,
thomas.wahl@uni-siegen.de

Citation:
Wahl, T., F. M. Calafat, and M. E. Luther (2014), Rapid changes in the seasonal sea level cycle along the US Gulf coast from the late 20th century, *Geophys. Res. Lett.*, *41*, 491–498, doi:10.1002/2013GL058777.

Received 21 NOV 2013
Accepted 27 DEC 2013
Accepted article online 3 JAN 2014
Published online 23 JAN 2014

Rapid changes in the seasonal sea level cycle along the US Gulf coast from the late 20th century

Thomas Wahl[1,2], Francisco M. Calafat[1,3], and Mark E. Luther[1]

[1]College of Marine Science, University of South Florida, St. Petersburg, Florida, USA, [2]Research Centre Siegen-FoKoS, University of Siegen, Siegen, Germany, [3]National Oceanography Centre, Southampton, UK

Abstract Temporal variations of the seasonal sea level harmonics throughout the 20th and early 21st century along the United States Gulf coast are investigated. A significant amplification of the annual sea level cycle from the 1990s onward is found, with both lower winter and higher summer sea levels in the eastern Gulf. Ancillary data are used to build a set of multiple regression models to explore the mechanisms driving the decadal variability and recent increase in the annual cycle. The results suggest that changes in the air surface temperature toward warmer summers and colder winters and changes in mean sea level pressure explain most of the amplitude increase. The changes in the seasonal sea level cycle are shown to have almost doubled the risk of hurricane induced flooding associated with sea level rise since the 1990s for the eastern and north-eastern Gulf of Mexico coastlines.

1. Introduction

The seasonal cycle is an energetic component in the sea level spectrum and dominates the intra-annual sea level variability outside the semidiurnal and diurnal tidal bands in most regions of the world. It consists of semi-annual and annual components, which are more or less pronounced depending on the geographic location [e.g., *Tsimplis and Woodworth*, 1994]. Despite containing a very small gravitational contribution [*Pugh*, 1987], the seasonal sea level cycle (SSLC) is primarily driven by meteorological and oceanographic processes, which are also responsible for considerable temporal variations. Changes in the annual or semi-annual amplitudes or phase lags have an immediate impact on marine coastal systems. Increases (or decreases) in the amplitudes or phase shifts toward (or away from) the storm surge season may for instance exacerbate (or reduce) the risk of coastal flooding and/or beach erosion. Changes in the SSLC may furthermore impact the health of ecological valuable and productive estuarine systems and coastal wetlands by altering the salt balance of intertidal sediments and, in turn, the primary production [e.g., *Morris*, 2000]. The temporal variability in coastal SSLC has mostly been examined at the regional scale, e.g., *Plag and Tsimplis* [1999] for the North and Baltic Sea, *Marcos and Tsimplis* [2007] for the Mediterranean Sea and the Atlantic Iberian coast, *Barbosa et al.* [2008] for the North Atlantic, *Hünicke and Zorita* [2008] for the Baltic Sea, *Barbosa and Silva* [2009] for Chesapeake Bay, *Dangendorf et al.* [2012, 2013] for the German Bight, and *Torres and Tsimplis* [2012] for the Caribbean Sea. A regional assessment for the Gulf of Mexico (GOM) has not yet been undertaken, although the widespread low lying areas along major parts of the coastline and sensitive ecosystems in shallow water regions are expected to be very susceptible to even small changes in the intra-annual sea level variability.

Here, we explore temporal changes in the seasonal sea level harmonics as derived from a set of 13 tide gauges (TGs) providing at least 30 years of data and covering much of the United States (US) GOM coastline. We use various ancillary data sets from the 20th century reanalysis project (20CR) [*Compo et al.*, 2011], as well as reconstructions of the sea surface temperature (SST) and steric sea level (ST) and develop simple and multiple linear regression models to understand the mechanisms driving the observed changes.

2. Data and Methods

Monthly mean sea level (MSL) time series from 13 TGs along the US GOM coastline are analyzed (Figure 1a). All records provide at least 30 years of data between 1900 and 2011 and at least 15 years for the period after 1990 (Figure 1b). The data sets were downloaded from the Permanent Service for Mean Sea Level (PSMSL) database. Gaps of one month were linearly interpolated (this correction affects less than 1% of the values at all sites) and years with two or more missing values were discarded from the analysis.

©2014. American Geophysical Union. All Rights Reserved.

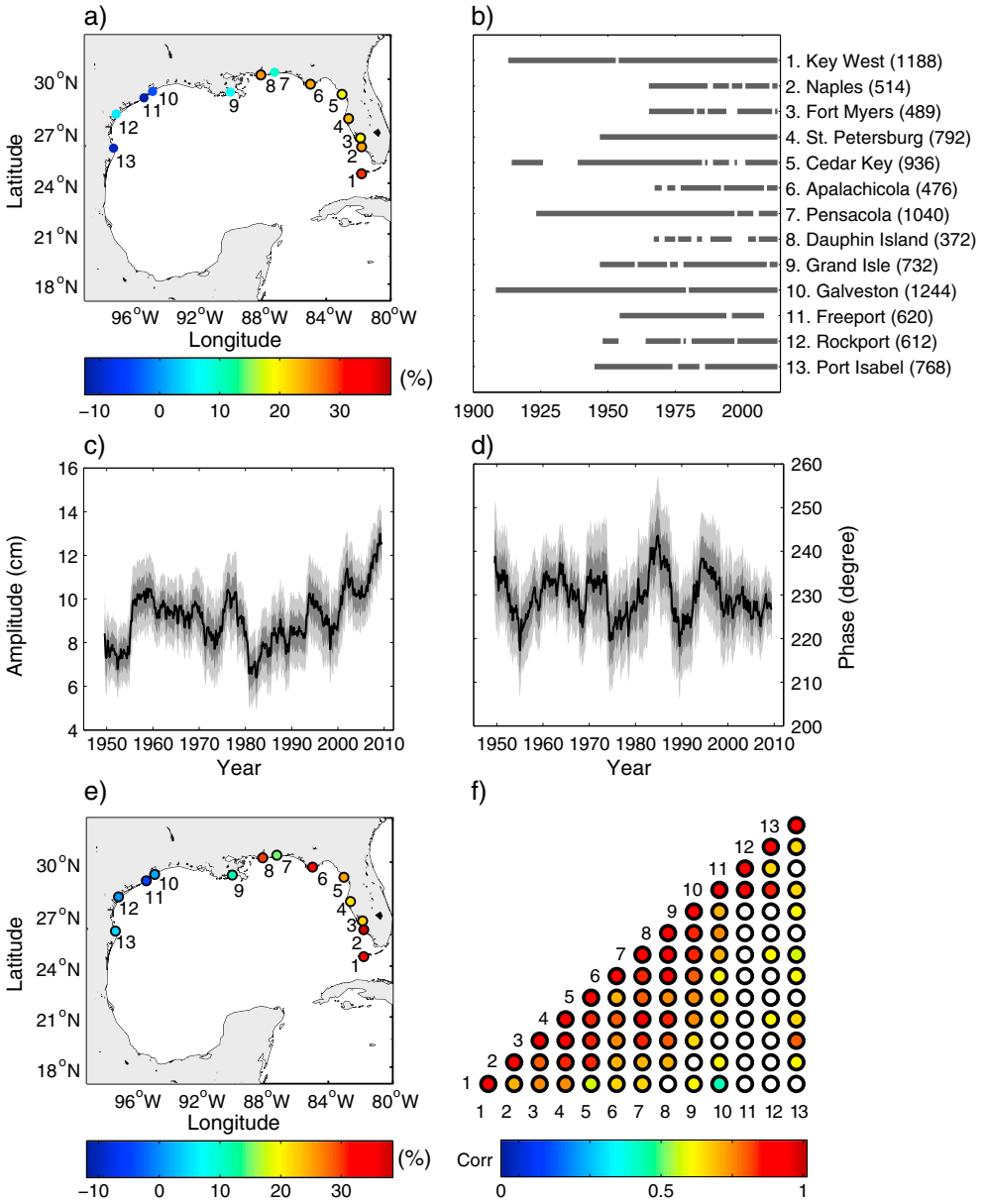

Figure 1. (a) Investigation area with TG sites and observed percentage changes of the annual amplitude of the SSLC (see text; black circles denote changes that are significant at the 68% confidence level). (b) Available data set lengths at the TGs. (c) and (d) Temporal changes in the annual amplitude and phase lag of the SSLC at the St. Petersburg tide gauge with 68% (dark grey) and 95% (light grey) confidence bands. (e) Percentage changes of the annual amplitude of the SSLC as reconstructed with the MLR_{IT} model. (f) Correlation matrix of the annual amplitude time series (5 year running windows) derived from the individual tide gauge records (TGs are numbered as in Figure 1b and circles were left blank when the correlation was not significant at the 95% confidence level according to a *t* test with the number of degrees of freedom reduced to account for the 5 year moving windows).

In order to explain the observed temporal changes in the SSLC we use monthly 2° × 2° global gridded atmospheric reanalysis data from the 20CR covering the period from January 1871 to December 2011, including air surface temperature (T), precipitable water (Prec), mean sea level pressure (MSLP), and zonal (u) and meridional (v) wind at 10 m. The 20CR data and a monthly 2° × 2° global gridded SST reconstruction (we use version 3b of the Extended Reconstructed Sea Surface Temperature, ERSST) from 1854 onward were downloaded from the National Oceanic and Atmospheric Administration (NOAA) website. The ST component of sea level was derived from monthly 1° × 1° global gridded temperature and salinity fields with 24 unevenly distributed vertical levels covering the upper 1500 m of the water column and spanning the period from 1945

©2014. American Geophysical Union. All Rights Reserved.

to 2011 (the data were downloaded from http://atm-phys.nies.go.jp/~ism/pub/ProjD/; we use version v6.12) [*Ishii and Kimoto*, 2009]. Since *Liu and Weisberg* [2012] highlighted that the upper layers (especially the first 100 m) contribute the major part to the ST variations within a year in the deep GOM, the ST was referenced to 200 m.

We calculate the temporal changes of the amplitudes and phase lags of the annual and semi-annual harmonics by fitting the following multiple regression to running 5 year windows of the time series of monthly MSL and the ancillary data sets [e.g., *Torres and Tsimplis*, 2012].

$$Z_0(t) = \overline{Z}_0 + at + A_1 cos\left[\frac{2\pi}{12}(t - \Phi_1)\right] + A_2 cos\left[\frac{2\pi}{6}(t - \Phi_2)\right] \quad (1)$$

In this regression, the monthly mean sea level (Z_0) is explained by a constant mean value ($\overline{Z}_0$), a linear trend (a), and annual and semi-annual cycles defined by their amplitudes (A_1 and A_2) and phase lags (Φ_1 and Φ_2); t is the time in months. The window is shifted by one month each time step; around data gaps, values are calculated when at least three years of data are available.

The temporal variation of the annual harmonics A_1 and Φ_1 derived from the TG record of St. Petersburg, Florida is presented in Figures 1c and 1d, respectively. Both variables show a considerable decadal variability and the amplitude also exhibits an increase since about 1990. A similar increase is not found in the annual phase lag which peaks in August (210 to 240 degrees) or September (240 to 270 degrees) and the semi-annual harmonics (see Figure S1 in the supplementary material). Hence, the focus of this present study is on analyzing and explaining the observed changes in the amplitude of the annual cycle.

First, increases similar to those found for St. Petersburg are sought in the remaining 12 tide gauge records. We compare the maximum values of the annual amplitudes before and after 1990 and apply a two sample t test to assess the significance of the difference between the two maximum values. In order to explore the mechanisms driving the variability in the SSLC we build regression models using the running 5 year annual amplitudes of the different variables described above as independent predictors and the running 5 year annual sea level amplitude A_1 as the dependent variable. Time series of the predictors are selected, for all 13 tide gauges, among the grid points located 4° × 4° around the TG sites as the one showing the highest correlation with the annual sea level amplitude time series. The ST component is the only exception to this rule. In this case we scan an area of 6° × 6° around the TG sites, searching for the time series with the smallest root mean square error (RMSE) when being compared to the sea level amplitude time series. Thereby, we assure that we find a grid point in deep water off the continental shelf, where the steric seasonal signal is fully developed and then projected as a mass component into the shallow coastal water regions [*Liu and Weisberg*, 2012].

The identified time series of the different variables are then used to build a set of multiple linear regression (MLR) models, starting with a base model MLR_{base}, where the relationship between the annual amplitude A_1 at a TG observed at a time t and the independent variables, $x_{t1}, x_{t2}, \ldots, x_{tp}$, is given by

$$A_{1t} = \mathbf{x}_t^T \beta + u_t, \quad t = 1, 2, \ldots, n \quad (2)$$

where ^{T} is the transpose, $\mathbf{x}_t = (1, x_{t1} = t, \ldots, x_{tp})^T$, $\beta = (\beta_0, \beta_1, \ldots, \beta_p)^T$ is a $(p+1)$-dimensional vector containing the regression coefficients, and u_t is an error term. We follow a step-down procedure to reduce multicollinearity in the models. First, all independent predictors are included and then sequentially discarded when the regression coefficients are not statistically significant at the 95% confidence level according to a t test. Thus, the number of independent predictors included in the MLR_{base} models varies from site to site. To quantify the unique contribution of each predictor to the explained variance, the particular predictor is removed from the base model and the reduction in the explained variance is determined. The contribution to the observed recent increase is assessed by constructing simple linear regression (SLR) models between each predictor and the sea level amplitude and by comparing the highest pre- and post-1990 values of the reconstructed sea level amplitude time series.

The MLR_{base} models do not account for interaction effects; the contribution of an independent predictor (e.g., x_{t1}) to the dependent variable A_{1t} may be stronger or weaker when one of the other independent predictors (e.g., x_{t2}) takes on a particular high or low value, i.e., the marginal contribution of x_{t1} is conditional on x_{t2} [e.g., *Jaccard et al.*, 1990]. An example is the interaction between MSLP and zonal wind at the St. Petersburg tide

©2014. American Geophysical Union. All Rights Reserved.

Table 1. Highest Observed Annual Amplitudes for the Pre- and Post-1990 Periods and the Years When These Occurred, Differences Between the Highest Values (Δ_{max}, Bold Values are Significant on the 68% Confidence Level), *p*-Values Derived From a Two Sample *t* Test, and Summer (S) and Winter (W) Trends of the Air Surface Temperature and Mean Sea Level Pressure for the Pre- and Post-1990 Periods

	$Max_{<1990}$		$Max_{>1990}$		Δ_{max}	*p*	T (deg/yr)				MSLP (hPa/yr)			
Station	cm	year	cm	year	%	-	$S_{<1990}$	$W_{<1990}$	$S_{>1990}$	$W_{>1990}$	$S_{<1990}$	$W_{<1990}$	$S_{>1990}$	$W_{>1990}$
Key West	9.5	1957	12.4	2009	**30**	0.04	0.05	0.05	0.14	0.02	−0.04	−0.15	−0.56	0.72
Naples	10.3	1987	12.9	2009	**25**	0.08	0.03	0.02	0.08	−0.06	0.00	−0.10	−0.58	0.78
Fort Myers	11.3	1976	13.6	2009	**20**	0.06	0.03	0.02	0.08	−0.06	−0.01	−0.16	−0.60	0.66
St. Petersb.	10.5	1958	13.0	2009	**24**	0.03	0.04	0.04	0.26	−0.07	0.00	−0.13	−0.59	0.70
Cedar Key	12.3	1978	14.6	2009	**19**	0.07	0.03	0.02	0.16	−0.27	0.05	−0.08	−0.68	0.68
Apalachic.	9.2	1970	11.4	2009	**25**	0.23	0.03	0.05	0.24	−0.02	0.05	−0.06	−0.67	0.72
Pensacola	11.6	1959	12.7	2003	10	0.53	0.01	−0.02	0.21	0.10	0.10	0.01	−0.65	0.67
Dauphin Isl.	9.8	1977	12.3	2009	**26**	0.21	0.01	−0.02	0.19	−0.06	0.09	0.04	−0.59	0.67
Grand Isle	11.1	1959	11.8	2009	7	0.66	0.03	0.07	0.32	−0.07	0.04	−0.02	−0.59	0.78
Galveston	11.0	1959	10.5	2009	−4	0.83	0.00	0.01	0.11	−0.18	0.09	0.23	−0.10	0.16
Freeport	10.3	1959	9.0	2001	−12	0.60	0.00	0.01	0.11	−0.18	0.02	0.16	−0.10	0.60
Rockport	8.9	1969	9.4	1996	5	0.87	0.00	0.01	0.11	−0.18	0.03	0.16	0.04	0.36
Port Isabel	9.3	1963	8.3	2008	−11	0.64	0.01	−0.10	0.10	−0.11	0.00	0.10	−0.03	0.39

gauge (see Figure S2 in the supplementary material). Such interactions, if not captured by the MLR model, may result in reduced model skill. Therefore, we build a second set of models adding first-order interaction terms, but only between the independent predictors that are still included in the base model after following the step-down procedure (i.e., we do not want to include interaction terms of predictors that have previously been identified to have insignificant regression coefficients). We note that including interaction terms also adds collinearity back to the model. However, at this stage we seek to improve the overall model skill rather than exploring the contributions of individual variables to the observed changes. In the model with interaction terms (MLR_{IT}), x_t in equation 2 is substituted by $x_t = (1,\ x_{t1} = t, \ldots, x_{tp},\ x_{t1}\ x_{t2}, \ldots, x_{tp-1}\ x_{tp})^T$. Again, we start by adding interaction terms between all independent predictors and then sequentially discard those with insignificant regression coefficients.

Finally, a third model MLR_{IT_ST} is built, which is similar to the MLR_{IT}, but without the steric component. The latter has only been available since 1945, while some of the TG records go back to the early 20th century. Hence, discarding the ST component allows us to reconstruct the annual amplitude over the entire record lengths at all sites.

The MLR models are first applied to all 13 TG records and then to two "index" time series, derived by averaging the annual sea level amplitude time series from two different sets of TGs (Key West to Grand Isle for the eastern GOM; Galveston to Port Isabel in the western GOM). Equal weight is given to all TGs as they are relatively equally distributed along the two coastline stretches.

3. Results

The results from analyzing the observed changes in the annual amplitude of the SSLC at all 13 TGs are summarized in Table 1. The highest values that have been observed in the pre- and post-1990 periods are displayed along with the central year of the 5 year window when the values occurred. In the pre-1990 period the highest values were observed in different years and decades across the sites, whereas for the post-1990 period the highest values occurred in 2009 (that is the central year of the last 5 year window considered here) at 9 of the 13 TGs. With the exception of Galveston, all of these sites are located in the eastern part of the GOM. In the same region the maximum values observed after 1990 were also higher than those found in the much longer (at most stations) pre-1990 period, indicating that a similar recent increase in the annual amplitude to that observed in St. Petersburg took place along the entire eastern GOM coastline. The differences between the post-1990 and pre-1990 values are expressed as percentages in Table 1 and are marked bold when they are significant at the 68% confidence level according to the two-sample *t* test; the respective *p*-values are also shown in the table. The increase in the annual amplitudes amounts to up to 30% and is significant at all stations along the coastline of West Florida, the Florida Panhandle (with the exception of Pensacola), and Dauphin

©2014. American Geophysical Union. All Rights Reserved.

Table 2. Contribution of Individual Predictors to the Explained Variance (EV) and the Recent Amplitude Increase Δ_{max} (Order of Values is EV|Δ_{max}; Results are Only Shown for Predictors Included in the MLR_{base} models) and the Results Derived With the Three MLR Models (N_{IT} is the Number of Interaction Terms Included in the MLR_{IT} Model)

	Individual Contribution														MLR_{base}		MLR_{IT}			MLR_{IT_ST}	
Station	T		SST		ST		MSLP		u		v		Prec		EV	Δ_{max}	N_{IT}	EV	Δ_{max}	EV	Δ_{max}
Key West	19	13	8	2	0	−1	1	5	1	1	4	4		–	52	21	12	70	32	51	25
Naples	21	26	9	5		–	7	25	12	−3		–	1	5	68	28	6	73	38	73	38
Fort Myers	4	36	4	9	1	2	10	31	0	1	2	13	0	4	84	30	9	92	23	88	23
St. Petersb.	14	26	1	6	0	1	0	10	6	−1	5	11		–	66	21	9	77	22	75	26
Cedar Key	10	9	3	2	1	1	1	5	5	0	4	7	3	6	71	13	12	84	26	79	19
Apalachic.	1	29	1	6	2	9	1	21	1	7	0	16	4	22	75	31	13	85	34	77	39
Pensacola	15	19		–		–	1	5	10	−2	3	2	1	7	65	14	7	72	15	62	24
Dauphin Isl.	5	37	2	3	2	0		–	2	14		–	5	26	85	38	5	88	30	86	33
Grand Isle		–	20	4		–		–	0	10		–	6	10	58	8	3	62	12	62	12
Galveston	13	−14		–	2	16		–	2	−4		–	11	17	76	6	3	80	2	68	21
Freeport		–		–	1	−7		–	4	−21	4	−10	19	17	74	−4	2	78	−5	76	−3
Rockport	4	5	3	−7	7	11	6	5		–	3	−2	12	23	70	16	5	73	0	65	7
Port Isabel	5	1		–	26	14	5	1	3	−3	2	−7	1	10	46	2	12	74	4	47	7

Island. Only small increases or even decreases are found for the TGs in the western GOM, but these are not significant. The percentage changes between the highest pre- and post-1990 values are also shown in Figure 1a providing a spatial picture and highlighting the regional differences between the eastern and western GOM.

The results from applying the SLR and different MLR models are summarized in Table 2. Results from assessing the contribution of individual predictors are only presented for those included in the MLR_{base} models after following the step-down procedure. At the majority of TGs, especially in the eastern GOM, the largest fraction of the observed variance can be explained by temporal fluctuations of T. Overall, the fraction of variance uniquely explained by individual predictors is small (compared to the MLR models discussed below), highlighting that the amount of variance commonly explained by several or all of the predictors is large.

The observed increase in the sea level amplitude in the eastern GOM can be largely explained by increases in the amplitudes of T and MSLP. Hence, these two variables are used to examine whether the sea level amplitude changes were driven by higher summer or lower winter sea levels or both. This approach is preferred here over calculating trends of monthly or seasonal MSL subseries and comparing these to the annual MSL trends. The latter are larger for the post-1990 period and may be influenced by asymmetric seasonal changes; higher summer and constant winter sea levels would for example introduce a positive MSL trend that is not part of the background signal we want to compare the seasonal trends to. T and MSLP time series, in contrast, do not show significant long-term trends at most sites in the region of interest and for the two time periods (pre- and post-1990). We note that there is still a small risk that long-term trends are masked or compensated by seasonal changes but the fact that the results are relatively coherent for both variables and across the TG sites supports the assumption that T and MSLP seasonal trends are not (or at least less) biased. The trends of T and MSLP for summer (August to October; i.e., when the annual sea level cycle peaks) and winter (February to April) are listed in Table 1 and reveal changes toward warmer summers and colder winters and lower MSLP in summer and higher MSLP in winter. All of these mechanisms lead to higher summer and smaller winter sea levels and are relatively symmetric on average across sites. Therefore, it can be assumed that the observed increase in the annual sea level amplitude in the eastern GOM was (almost) equally driven by higher summer and smaller winter sea levels. These seasonal changes are superimposed onto the global long-term background sea level rise attributed to both greenhouse warming and natural climate variability [e.g., *Calafat and Chambers*, 2013].

It is striking from Table 2 that the upper ST and SST explain much less of the observed variability and recent increase than T (especially in the eastern GOM). The time series of all three variables as used in the MLR models for the St. Petersburg tide gauge are shown in Figure S3 in the supplementary material highlighting that T is the only parameter with an amplitude increase similar to the one observed in sea level. The differences between the variables may be related to strong currents in the region associated with the Loop

©2014. American Geophysical Union. All Rights Reserved.

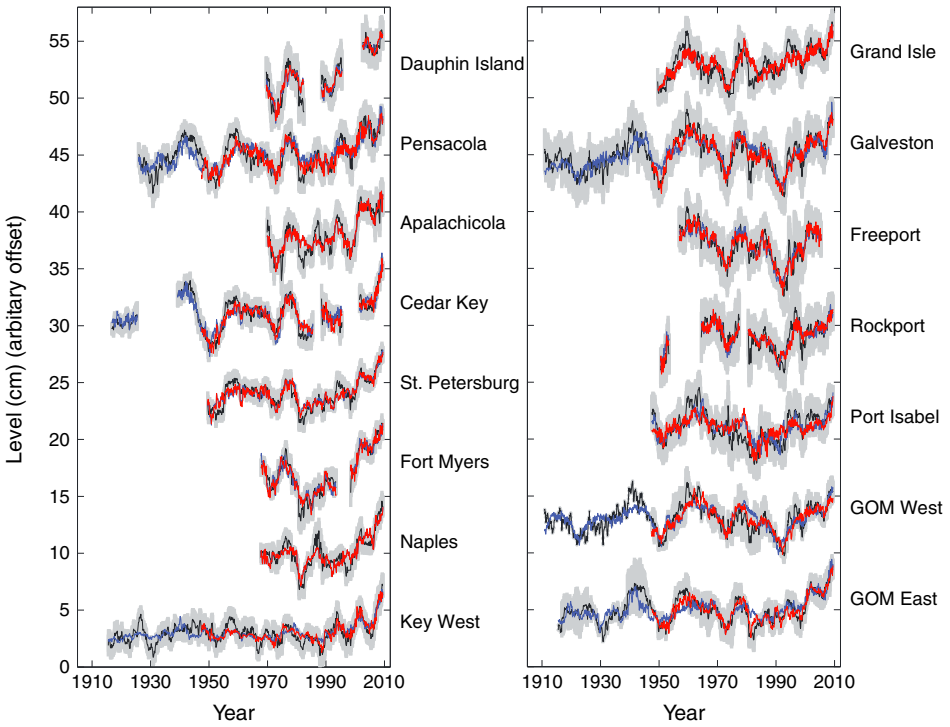

Figure 2. Observed (black) and reconstructed (red: MLR_{IT} model; blue: MLR_{IT_ST} model) time series of the annual amplitude of the SSLC (5 year running windows as described in the text) at the 13 TG sites and for two index time series representative of the western and eastern GOM, respectively. For the individual TGs, shaded bands represent 95% confidence levels of the observed amplitudes; for the index time series, shaded bands represent the standard deviations of the amplitude values (from individual TGs) averaged into the index.

Current; if the hydrographic data at the grid point where the ST is computed include profiles that happen to be on the eastern side of the Loop Current in the southward flow, their information may not be representative of the variability observed by the tide gauge. A contribution from steric changes below the reference level of 200 m may also explain part of the differences between T and ST. However, referencing ST to 700 m did not change the results and for deeper layers the profiles are too sparse. Oceanic heat advection, either horizontal or vertical, can lead to differences between T and SST and it is well known that these variables differ considerably in regions where strong currents prevail [e.g., *Singh et al.*, 2005]. Either way, examining the mechanisms behind the observed differences between T, SST, and ST in detail is beyond the scope of this study.

The MLR_{base} models for the 13 TGs were comprised of the independent predictors that have numbers in the "Individual Contribution" column of Table 2. On average, the models explain 68% of the observed variance, ranging from 46% in Port Isabel to 85% in Dauphin Island. The average of the reconstructed increase at the TG sites in the eastern GOM (from Key West to Grand Isle) is 23% compared to the observed increase at the same stations of 21%. By adding a varying number of interaction terms (N_{IT}) to the MLR_{IT} models, the explained variance increases to 77% on average, ranging from 70% in Key West to 92% in Fort Myers. The modeled increase in the sea level amplitude also becomes larger (26% on average) resulting in a slight over estimation. However, the spatial pattern with the distinct differences between the western and eastern GOM is well captured by the models (see Figure 1e). The reconstructed (with the MLR_{IT} model) and observed time series of the annual sea level amplitude are shown in Figure 2 as red and black solid lines, respectively. The reconstructed time series correspond well with the observed time series at all sites; the correlation between the two sets of time series ranges from 0.70 to 0.96.

Figure 2 also shows annual sea level amplitude time series for two "indices" being representative of the eastern (Key West to Grand Isle) and western (Galveston to Port Isabel) GOM regions. The selection of the tide gauge sets averaged into the two indices was based on the observed increase in the amplitude in the eastern GOM and its absence in the western part, as well as on the correlation matrix shown in Figure 1f. The latter highlights that most of the amplitude time series from TGs in the eastern GOM are highly correlated with

©2014. American Geophysical Union. All Rights Reserved.

each other but not with time series from the western GOM. The index for the eastern GOM is subject to less decadal variability and shows a marked increase toward the end of the time series leading to the highest values observed over the last century.

The third model MLR_{IT_ST} is the same as MLR_{IT}, but without the steric component as a predictor. This allows us to reconstruct the observed temporal changes over the entire lengths of the TG records. Discarding the ST component results in a reduction of the observed variance (70% on average; note that the values for the explained variance are not directly comparable to those derived with the two other models because at some TGs much longer time series are reconstructed and compared to the observations). It has, however, only negligible impact on the ability of the models to reproduce the recent increase in the annual sea level amplitude (see blue solid lines in Figure 2). The reconstructed time series still match the observed time series well and the correlation only decreases slightly, ranging from 0.68 to 0.94.

4. Discussion and Conclusions

We used tide gauge observations, atmospheric reanalysis data, and reconstructions of the SST and upper ST to investigate temporal changes in the SSLC along the US GOM coastline. We find a significant increase in the annual amplitude from the 1990s onward of up to 30% (21% on average) at virtually all TGs in the eastern GOM. The MLR models explain up to 92% of the observed variability at the TG sites (77% on average) when interaction terms are included and they are also capable of reconstructing the observed amplitude increase from the early 1990s onward.

Seasonal trends of T and MSLP (the two variables being mainly responsible for the amplitude increase) suggest that both higher summer and smaller winter sea levels contributed to the increase. Such seasonal changes, when superimposed onto the ongoing long-term sea level rise and the associated interannual to multidecadal fluctuations can have significant implications for the coastal flood risk and the health of marine ecosystems along the shallow GOM coastline and the connected estuaries. For the 1993 to 2011 period global MSL rise was estimated to be 3.2 ± 0.4 mm/yr from satellite measurements and 2.8 ± 0.4 mm/yr from coastal TGs [*Church and White*, 2011]. The latter can be translated into an absolute value of approximately 5 cm of sea level rise from 1993 to 2011. Taking the long record of Key West as an example, the annual amplitude of the SSLC for the most recent 5 year window was 12.4 cm, that is 4.5 cm (or 57%) higher than the long-term average prior to 1993. Assuming that this increase was equally driven by higher summer and lower winter sea levels, it can be concluded that the seasonal changes over the last approximately 20 years have led to summer base water levels upon which hurricane surges can built almost 90% higher as would be expected from global sea level rise alone (note that the amplitude is defined here as the "peak amplitude", i.e., the deviation from the mean). The second half of the amplitude changes, on the other hand, driven by lower winter sea levels, reduced the flood risk associated with winter storm surges. Such events, although not as common and usually less extreme than hurricane surges, also pose a considerable risk for coastal communities around the GOM as highlighted by the damages induced by the "Storm of the Century" in 1993 [e.g., *Kocin et al*., 1995].

Most of the independent predictors used for the MLR models presented here (especially for the MLR_{IT_ST} model) are output variables of climate models. The MLR models can thus also be used to infer information on possible future changes in the seasonal sea level cycle in the GOM and how this may affect the risk of coastal flooding and other associated variables.

Acknowledgments

T. Wahl was supported by a fellowship within the postdoctoral program of the German Academic Exchange Service (DAAD). F. M. Calafat was supported under a Marie Curie International Outgoing Fellowship (IOF) within the 7th European Community Framework Program (grant agreement PIOF-GA-2010-275851). Sönke Dangendorf and Steven Meyers provided helpful comments on an early draft of the manuscript. We also thank Ivan Haigh and Marta Marcos, whose comments/suggestions helped improving the quality of the paper.

The Editor thanks Ivan Haigh and Marta Marcos for assistance evaluating this manuscript.

References

Barbosa, S. M., and M. E. Silva (2009), Low-frequency sea-level change in Chesapeake Bay: changing seasonality and long-term trends, *Estuarine Coastal Shelf Sci.*, *83*, 30–38, doi:10.1016/j.ecss.2009.03.014.

Barbosa, S. M., M. F. Silva, and M. J. Fernandes (2008), Changing seasonality in North Atlantic coastal sea level from the analysis of long tide gauge records, *Tellus*, *60A*, 165–177, doi:10.1111/j.1600-0870.2007.00280.x.

Calafat, F. M., and D. P. Chambers (2013), Quantifying recent acceleration in sea level unrelated to internal climate variability, *Geophys. Res. Lett.*, *40*, 3661–3666, doi:10.1002/grl.50731.

Church, J. A., and N. J. White (2011), Sea-level rise from the late 19th to the early 21st century, *Surv. Geophys.*, *32*, 585–602, doi:10.1007/s10712-011-9119-1D.

Compo, G. B., et al (2011), The twentieth century reanalysis project, *Q. J. R. Meteorol. Soc.*, *137*, 1–28, doi:10.1002/qj.776.

Dangendorf, S., T. Wahl, H. Hein, J. Jensen, S. Mai, and C. Mudersbach (2012), Mean sea level variability and influence of the North Atlantic Oscillation on long-term trends in the German Bight, *Water*, *4*(1), 170–195, doi:10.3390/w4010170.

©2014. American Geophysical Union. All Rights Reserved.

Dangendorf, S., C. Mudersbach, T. Wahl, and J. Jensen (2013), Characteristics of intra-, inter-annual and decadal variability and the role of meteorological forcing: the long record of Cuxhaven, *Ocean Dyn.*, *63*(2-3), 209–224, doi:10.1007/s10236-013-0598-0.

Hünicke, B., and E. Zorita (2008), Trends in the amplitude of Baltic Sea level annual cycle, *Tellus*, *60A*, 154–164.

Ishii, M., and M. Kimoto (2009), Reevaluation of historical ocean heat content variations with time-varying XBT and MBT depth bias corrections, *J. Oceanogr.*, *65*, 287–299.

Jaccard, J., R. Turrisi, and C. K. Wan (1990), *Interaction effects in multiple regression*, Sage University Paper series on quantitative applications in the social sciences, 07-069, Sage, Newbury Park, Calif.

Kocin, P. J., P. N. Schumacher, R. F. Morales Jr., and L. W. Uccellini (1995), Overview of the 12-14 March 1993 superstorm, *Bull. Am. Meteorol. Soc.*, *76*(2), 165–182.

Liu, Y., and R. H. Weisberg (2012), Seasonal variability on the West Florida Shelf, *Prog. Oceanogr.*, *104*, 80–98, doi:10.1016/j.pocean.2012.06.001.

Marcos, M., and M. N. Tsimplis (2007), Variations of the seasonal sea level cycle in southern Europe, *J. Geophys. Res.*, *112*, C12011, doi:10.1029/2006JC004049.

Morris, J. T. (2000), Effects of sea level anomalies on estuarine processes, in *Estuarine science: A Synthetic Approach to Research and Practice*, edited by J. Hobbie, pp. 107–127 , Island Press, Washington, D. C., USA.

Plag, H. P., and M. N. Tsimplis (1999), Temporal variability of the seasonal sea-level cycle in the North Sea and Baltic Sea in relation to climate variability, *Global Planet. Change*, *20*(2–3), 173–203, doi:10.1016/S0921-8181(98)00069-1.

Pugh, D. T. (1987), *Tides, Surges and Mean Sea Level*, pp. 488, John Wiley, Chichester, U.K.

Singh, R., C. M. Kishtawal, and P. C. Joshi (2005), Estimation of monthly mean air-sea temperature difference from satellite observations using genetic algorithm, *Geophys. Res. Lett.*, *32*, L02807, doi:10.1029/2004GL021531.

Torres, R. R., and M. N. Tsimplis (2012), Seasonal sea level cycle in the Caribbean Sea, *J. Geophys. Res.*, *117*, C07011, doi:10.1029/2012JC008159.

Tsimplis, M. N., and P. L. Woodworth (1994), The global distribution of the seasonal sea level cycle calculated from coastal tide gauge data, *J. Geophys. Res.*, *99*(C8), 16,031–16,039, doi:10.1029/94JC01115.

©2014. American Geophysical Union. All Rights Reserved.